Appl. Phys. B 76, 717–720 (2003)
DOI: 10.1007/s00340-003-1171-1

Applied Physics B
Lasers and Optics

E. GEHRIG✉
O. HESS

High-frequency modulation of segmented-contact semiconductor lasers

Advanced Technology Institute, School of Electronics and Physical Sciences, University of Surrey, Guildford, Surrey, GU2 7XH, UK

Received: 14 January 2003/Revised version: 9 April 2003
Published online: 6 June 2003 •

ABSTRACT Simulations of the high-frequency modulation characteristics of semiconductor lasers with segmented contacts predict a pronounced resonance-like modulation response that is beyond five times the original cut-off modulation frequency. Based on an effective multi-mode Maxwell–Bloch model, the simulations reveal the underlying phenomena. They show that the high-frequency response is a direct consequence of the particular spatio-temporal and multi-mode dynamics induced by the segmented-contact laser geometry.

PACS 42.55.Px; 42.55.Ah

1 Introduction

One of the limiting factors in high-speed applications of semiconductor lasers is the well-known cut-off frequency in response to high-frequency injection-current modulation [1]. This is closely related to the internal carrier dynamics, that is, the times-scales of inter- or intraband relaxation and scattering. Those are generally accepted to be mainly material dependent. It would thus be of great technological relevance to find and explore avenues of circumventing these constraints, e.g. by mode-locking [2], multi-section lasers [3] or nonlinear intracavity interaction [4].

Encouraged by recent investigations on modulated semiconductor laser arrays [5, 6] we present here results of spatio-temporal simulations on high-frequency modulation characteristics of semiconductor lasers that have been modified with respect to the realization of their current contacts. We show that, indeed, a lateral segmentation of the contact(s) may, with proper asymmetric application of the injection current, lead to a more than five-fold increase of the modulation band-width. The simulations on the basis of Maxwell–Bloch equations reveal that the increased high-speed modulation is closely associated with the coupled lateral and longitudinal multi-mode dynamics of the laser.

2 Multi-mode Maxwell–Bloch equations

Generally, the high-speed dynamics of semiconductor lasers is determined by a complex interplay of ultrafast light-field and carrier-dynamics [7]. In order to theoretically describe and simulate these dynamics, propagation effects and spatio-temporally varying mode competition have to be taken into account. Here we present a multi-mode Maxwell–Bloch description for the theoretical analysis and numerical simulations of the high-speed modulation dynamics of longitudinally and/or transversely multi-segmented semiconductor lasers. Due to the explicit inclusion of longitudinal modes, and due to the consideration of transverse light field and carrier dynamics, the model allows the self-consistent inclusion of the coexistence and dynamic interplay of many transverse and longitudinal modes responsible for, for example, the laser-response.

In the following, we will concentrate on the most simple realization of a transversely segmented-contact laser: the twin-stripe laser. Figure 1 schematically shows its typical geometry. The active area consists of two stripes that are arranged parallel to each other on the device. The stripes have a lateral width w and a lateral distance d. L is the length of the device. Typically the lateral extension of the individual stripes is similar to the width of single stripe lasers, that is, approximately 3–5 μm. The length of the laser varies from a few hundred μm up to the mm-regime. The lateral distance of the stripes represents the most critical parameter. Its value (2–20 μm) is most relevant for the transverse coupling of the stripes and consequently for the spatio-temporal dynamics of the multi-stripe laser.

The multi-mode Maxwell–Bloch equations consist of spatially dependent multi-mode wave equations and a two-level Bloch description for the active semiconductor medium. The Bloch equations for a two-level homogeneously broadened medium model the complex material polarization and carrier density interacting with the propagating optical fields. The two-level approach allows efficient modeling of the relevant dynamic internal laser effects, such as diffraction, self-focusing, dynamic local-carrier generation, and carrier recombination by stimulated emission. However, we would like to note that the model is not appropriate for the simulation of microscopic carrier effects, such as carrier-heating, highly nonlinear carrier distributions, phonon dynamics, or many-body effects. The dynamic spatio-temporal interplay of longitudinal modes that is important for the long-time emission dynamics (relaxation oscillations, dynamic instabilities, and self-pulsations) and, in particular, the spatio-temporal dynam-

✉ Fax: +44-1483/68-6081, E-mail: e.gehrig@surrey.ac.uk

ics of modulated lasers, is included via a multi-mode expansion of the fields:

$$P = e^{\mathrm{i}kz}\sum_n P^+_{(n)}e^{2\mathrm{i}nkz} + e^{-\mathrm{i}kz}\sum_n P^+_{(n)}e^{-2\mathrm{i}nkz}\,,$$
$$N = N_0 + \sum_n \left(N^+_{(n)}e^{2\mathrm{i}nkz} + \text{c.c.}\right)\,. \tag{1}$$

Inserting the multi-mode expansion of the light in Maxwell's wave equations, the equations for the dynamics of the light fields propagating in the forward ('+') and backward ('−') directions within the laser read

$$\frac{\partial}{\partial t}E^\pm + \frac{\partial}{\partial z}E^\pm = \mathrm{i}D_\mathrm{p}\frac{\partial^2}{\partial x^2}E^\pm - \mathrm{i}\eta E^\pm + \Gamma P^\pm_{(0)}\,, \tag{2}$$

where $P^\pm_{(0)}$ is the lowest order coefficient of the mode expansion of the polarization. The diffraction coefficient is $D_\mathrm{p} = (2n_l k_0)^{-1}$, with the vacuum wavenumber $k_0 = 2\pi/\lambda$. The waveguiding properties derived from the effective index approximation are included in the parameter η. Γ is the confinement factor. Via the polarization the light fields are locally coupled to carriers within the active medium. On the basis of an effective two-level description of the material properties of the active medium, the dynamics of the carrier density and the polarization can be described by the following Bloch equations:

$$\begin{aligned}
\frac{\partial}{\partial t}P^\pm_{(0)} &= -\gamma_\mathrm{p}\left[\left(1+\mathrm{i}\frac{\bar\omega}{\gamma_\mathrm{p}}\right)+(\varrho+\mathrm{i}\sigma)\,N\right]P^\pm_{(0)} \\
&\quad +\beta\left(\left(N_{(0)}+\mathrm{i}\alpha\right)E^\pm + N_{(1)}E^\mp\right)\,, \\
\frac{\partial}{\partial t}P^\pm_{(1)} &= -\gamma_\mathrm{p}\left[\left(1+\mathrm{i}\frac{\bar\omega}{\gamma_\mathrm{p}}\right)+(\varrho+\mathrm{i}\sigma)\,N\right]P^\pm_{(1)} + \beta N_{(1)}E^\pm\,, \\
\frac{\partial}{\partial t}N_{(0)} &= \Lambda + D_\mathrm{f}\nabla^2 N_{(0)} - \gamma_\mathrm{nr}N_{(0)} \\
&\quad -2\Big(E^+\left(P^+_{(0)} - \Lambda_0 E^+\right)^* \\
&\quad +E^-\left(P^-_{(0)} - \Lambda_0 E^-\right)^* + \text{c.c.}\Big)\,, \\
\frac{\partial}{\partial t}N_{(1)} &= -4D_\mathrm{f}k_z^2 N_{(1)} - \gamma_\mathrm{nr}N_{(1)} \\
&\quad -2\Big(E^+\left(P^-_{(0)} - \Lambda_0 E^-\right)^* + E^{-*}\left(P^+_{(0)} - \Lambda_0 E^+\right) \\
&\quad +E^{+*}P^+_{(1)} + E^- P^{-*}_{(1)}\Big)\,.
\end{aligned} \tag{3}$$

In (3) the pump term Λ describes the carrier injection into the stripes. The parameters $P_{(0)}$, $P_{(1)}$, $N_{(0)}$, and $N_{(1)}$ are the (lowest order) coefficients of the mode-expansion. D_f is the carrier diffusion constant and k_z denotes the wavenumber of the propagating light fields. $\bar\omega$ denotes the frequency detuning between the frequency of the electron–hole pair and the light frequency. γ_nr is the rate of nonradiative recombination and γ_p describes the dephasing of the dipole. The dimensionless constant β determines the maximum gain. The material parameters ϱ and σ consider the increase in the polarization decay rate and the drift of the gain maximum with increasing carrier density, respectively. The α-factor (α) describes the amplitude phase coupling. The parameter Λ_0 guarantees a vanishing gain at transparency. Typical values for these parameters can be found in [8].

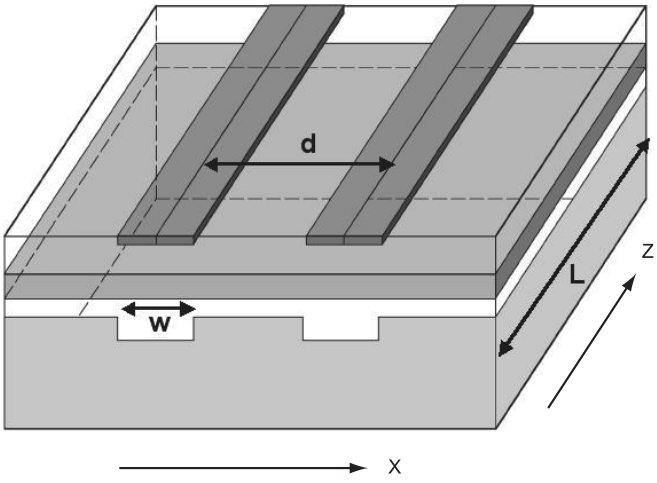

FIGURE 1 Schematic geometry of a twin-stripe laser. The width of the individual stripes is w and their lateral distance is d. L denotes the length of the structure

3 High-frequency modulation dynamics

In order to analyze the 'response' of the laser to current-modulation we have varied the modulation frequency of the pump term and calculated the resulting spatio-temporal behavior of the near-field and the carrier inversion. The simulation results depicted in Fig. 2 visualize the temporal behavior of the current-modulated two-segment laser (with average current density $j = 1.3\,j_\mathrm{thr}$) for modulation frequencies of (a, d) 2, (b, e) 4, and (c, f) 6 GHz. The upper and lower rows show the dependence of the emitted intensity and the corresponding current density on time, respectively. In the case of the 2-GHz modulation (Fig. 2 a and d) one can observe a profound and regular modulation of the carrier density. The modulations of the current are sufficiently slow that the carrier inversion (Fig. 2d) can follow (that is, within one period and before the start of the next peak). The resulting gain modulation leads to emission of a regular pulse train displayed in Fig. 2a. With increasing modulation frequency, the pulses are emitted more and more out of phase. Irregular and spatio-temporally broadened pulses appear instead (Fig. 2c). This behavior is a direct consequence of the finite material-dependent interaction times that govern the dynamics of the laser: spontaneous and induced emission leading to spatio-temporal hole burning and the re-establishment of the gain via the pump current have characteristic time scales ranging from the ps up to the ns regime. For high-speed modulation (i.e. > 2 GHz) the carrier density can no longer follow fast enough due to the finite interaction times. As a consequence the modulation of the inversion is 'smeared out' (Fig. 2f), leading to irregular pulse emission (Fig. 2c). Indeed, this cut-off frequency marks the relaxation oscillation and usually represents a modulation limit for a narrow-stripe single-contact semiconductor laser. In spatially extended semiconductor lasers, however, the longitudinal and transverse dimensions generally enable the coexistence of numerous longitudinal and transverse modes. With suitable resonator design allowing segmented-contact

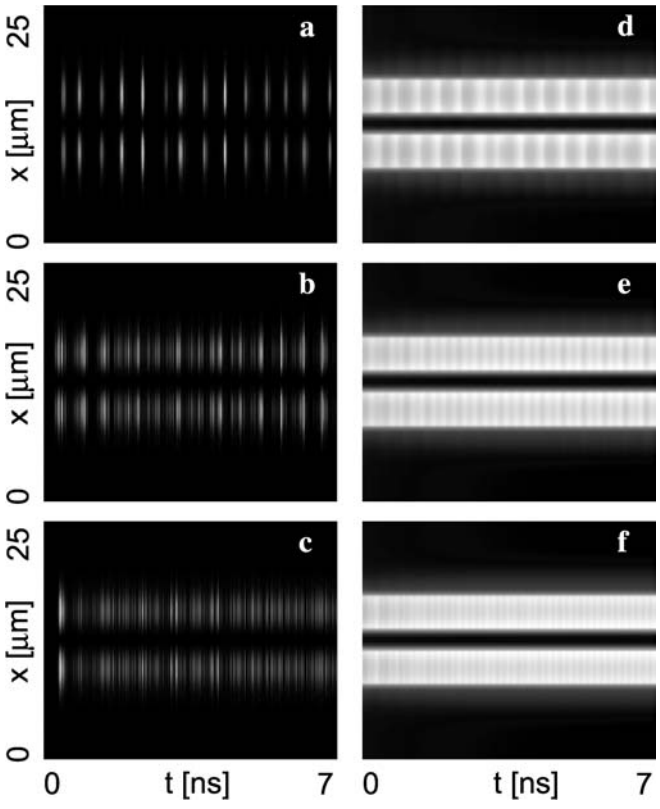

FIGURE 2 Dependence of the near-field intensity (**a**–**c**) and the carrier density (**d**–**f**) of a semiconductor laser with segmented contacts (segment separation 2 µm) on modulation frequency. The frequency of the current modulation is 2 (**a**, **d**), 4 (**b**, **e**), and 6 GHz (**c**, **f**). The (average) current density is $j = 1.3\, j_{\mathrm{thr}}$

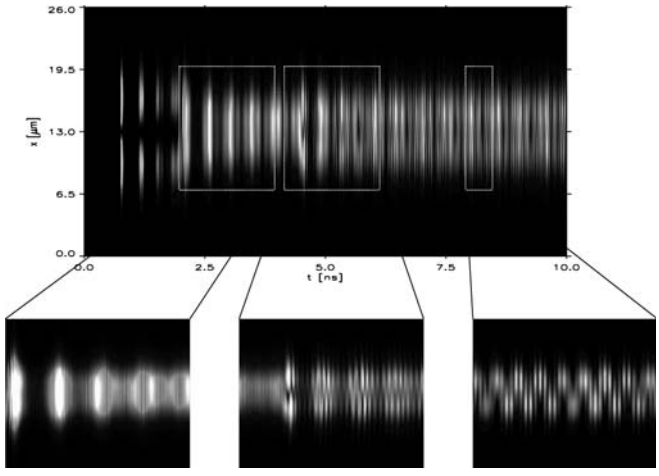

FIGURE 3 Spatio-temporal dynamics of the near-field intensity of a segmented-contact semiconductor laser. In the *lower* graphs, sections indicated by *dotted lines* are magnified. The high-speed modulated current is applied with a modulation frequency of 8 GHz to one of the segments while the second segment is pumped with continuous current. The separation between the contact segments is 2 µm with an average injection current of $j = 2.0\, j_{\mathrm{thr}}$ applied to both contact segments

carrier injection and modulation it should thus be possible to directly influence the lateral coupling and transverse mode dynamics of a given laser structure and modulate the laser with a beat frequency associated with these modes. By application of a sufficiently high current (leading to increased carrier diffusion and interaction of evanescent waves between the two stripes) and, in particular, using the method of asymmetric modulation (i.e. only modulating one of the two stripes), we can increase the transverse dynamics of the light fields. If, in addition, the modulation frequency corresponds to the transverse light-field migration, the laser may show a strong laser response. Indeed, as the example in Fig. 3 demonstrates, a spatially inhomogeneous high-speed modulation leads to a pronounced response of the two-segment laser at a modulation frequency of 8 GHz that is far beyond the former cut-off frequency of 2 GHz. The average injection current density is $j = 2.0\, j_{\mathrm{thr}}$ in both stripes. The sine-shaped modulation is only applied to the lower stripe. The modulation of the carrier inversion in the lower stripe is via the light diffraction and the nonlinear interaction of the evanescent waves partially transferred to the second (upper) stripe. The resulting laterally inhomogeneous pump profile leads to an increased lateral migration of the light fields that ends up in the excitation of a transverse eigenmode of the laser. The time-window displayed in Fig. 3 and, in particular, the magnified time-traces depicted below demonstrate a sequence of different characteristic regimes experienced by the laser until a quasi-stationary regime is reached. Immediately after turning on the current (0–2 ns), the stripes show individual pulsations. After some time the coupling lateral modes leads, in combination with the light propagation, to increasing interaction. First, at 2–4.5 ns, lateral modes merge and show an emission behavior similar to a single laser stripe. Then, the synchronized pulsations induced by the mutual interaction of light and matter in combination with the laterally inhomogeneous carrier injection leads to the gradual formation of a transverse dynamics (4.5–6 ns). In its final state (~ 6 ns), the laser shows a regular transverse migration of the light that can be identified with a higher-order transverse mode. The time for two left–right changes of the intensity (belonging to the positive and negative phases of the respective light fields) thereby corresponds to the frequency of the modulation (8 GHz).

Figure 4 shows the result of a systematical variation of the modulation frequency and subsequent calculation of the response of the laser. Every point of the modulation response curve is the result of a spatio-temporally resolved simulation with the respective current modulation. The intensity values are via $I(z = L) \propto \left(\mathrm{Re}[d_{\mathrm{cv}} E(z = L)]^2 + \mathrm{Im}[d_{\mathrm{cv}} E(z = L)]^2\right)$ related to the dynamically calculated optical fields at the output facet ($z = L$). The temporally averaged (over 20 ns) intensity values are spatially averaged over the transverse (x) coordinate of the laser, leading to the individual points of the curve (in logarithmic scale). In the case of the grey response curve the parameters were chosen identically to the situation of Fig. 3. For the black line the current amplitude of one of the stripes was increased by a factor of 1.05. We note that each point of the curve is the result of the full spatio-temporally resolved calculation of the light fields within the framework of the multi-mode Maxwell–Bloch equations.

The modulation curve shows a first peak near 2 GHz corresponding to the typical laser-internal interaction times determined by the build-up and decay of inversion and intensity. Increasing the modulation frequency then leads to a dramatic decrease of the response. This effect is caused by the limitations from the dynamics of the inversion,

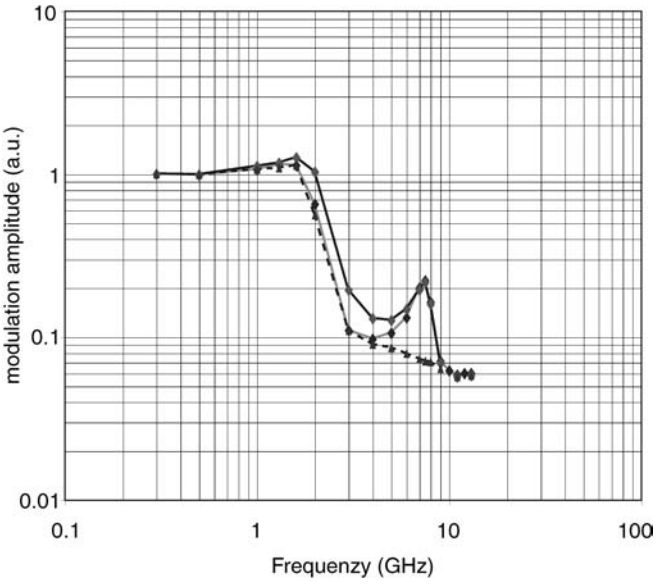

FIGURE 4 Modulation response of a semiconductor laser with homogeneous (*circles*, *dashed line*) and segmented (*diamonds*, *full grey* and *black lines*) contacts. The *grey line* corresponds to identical current amplitudes in both stripes, and the *black line* corresponds to a simulation in which the current amplitude in one of the stripes was increased by a factor of 1.05

which cannot follow the instantaneous injection current within a modulation period. In the high-frequency regime, near 8 GHz, a second maximum can be observed. This directly corresponds to the excitation of a transverse mode (cf. Fig. 3) and high-frequency out-of-phase oscillation. This notion is further supported by the change seen in the modulation response (Fig. 4, black line) resulting from an increase of the modulation amplitude of the modulated current.

For a more detailed analysis of the high-speed laser response, Fig. 5 shows a part of the transversely (x) resolved spectrum (ω) of the twin-stripe laser. The spectrum shows the transverse modes belonging to one longitudinal mode. In the twin-stripe laser the longitudinal modes split for sufficiently high injection currents into two transverse modes corresponding to the lateral eigenmodes of the system. Their spectral offset is a result of the coupled longitudinal and transverse light-field dynamics in the laser resonator. It strongly depends on the width of the two stripes, the stripe separation and, due to the coupling of longitudinal and transverse degrees of freedom, on the cavity length. In principal the relationship between width and length of the laser determines the spectral range of the transverse modes, whereas boundary conditions such as the amplitude of the current in the two stripes and the reflectivities of the facets define the "sharpness" of the curve. The displayed mode separation of 8 GHz reveals that the driving of a twin-stripe laser with a modulated current is particular sufficient if the modulation frequency "fits" the mode separation of these two eigenmodes.

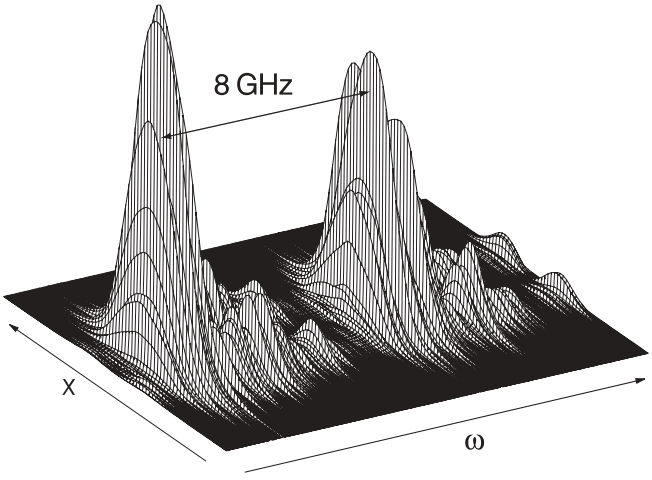

FIGURE 5 Mode-splitting of a longitudinal mode occurring during high-frequency modulation

4 Conclusion

In conclusion, we have studied the high-speed modulation dynamics of segmented-contact semiconductor lasers. Simulations on the basis of a multi-mode Maxwell–Bloch theory predict the existence of a narrow-band high-frequency modulation resonance near 8 GHz that broadens with increasing current. The simulations show that the high-speed characteristics can be attributed to the dynamic lateral coupling of the stripes, as well as to the spatio-temporal coupling of transverse and longitudinal degrees of freedom. The multi-mode Maxwell–Bloch theory thus represents a fundamental basis for the control of the mode dynamics and for the exploration and design of the high-speed modulation characteristics of semiconductor lasers that may be integrated into high-speed optical communication systems.

REFERENCES

1 R. Olshansky, P. Hill, V. Lanzsiera, W. Pawazinik: IEEE J. Quantum Electron. **QE-23**, 1410 (1987)
2 E. Goutain, J.C. Renaud, M. Krakowski, D. Rondi, R. Blondeau, D. Decoster: Electron. Lett. **32**, 896 (1996)
3 K.Y. Lau: IEEE J. Quantum Electron. **QE-26**, 250 (1990)
4 R. Nietzke, W. Elsäßer, A.N. Baranov, K. Wünstel: Appl. Phys. Lett. **56**, 554 (1991)
5 H. Lamela, B. Roycraft, P. Acedo, R. Santos, G. Carpintero: Opt. Lett. **27**, 303 (2002)
6 G. Carpintero, H. Lamela, M. Leones, C. Simmendinger, O. Hess: Appl. Phys. Lett. **78**, 4097 (2001)
7 W.W. Chow, S.W. Koch, M. Sargent III: *Semiconductor-Laser Physics* (Springer-Verlag, Berlin, Heidelberg 1994)
8 E. Gehrig, O. Hess: *Spatio-Temporal Dynamics and Quantum Fluctuations in Semiconductor Lasers* (Springer, Heidelberg 2003)